

# Electron-hole recombination lifetimes in a quasi-zero-dimensional electron system in $\text{CdS}_x\text{Se}_{1-x}$

Kai Shum, G. C. Tang, Mahesh R. Junnarkar, and R. R. Alfano

*Institute for Ultrafast Spectroscopy and Lasers, Departments of Electrical Engineering and Physics, The City College of New York, New York, New York 10031*

(Received 1 December 1986; accepted for publication 25 September 1987)

The recombination lifetimes for the radial and angular quantum number conserved  $1S-1S$  and  $1P-1P$  transitions from three-dimensionally confined electrons in  $\text{CdS}_x\text{Se}_{1-x}$  were measured by time-resolved photoluminescence (PL). The assignment of the observed transitions was supported by calculations of eigen energy levels and squared matrix element ratio for these transitions as well as well-resolved PL peaks arising from  $1S-1S$  and  $1P-1P$  transitions.

Recently, carriers localized in semiconductor microstructures have attracted much attention because of their novel optical properties for potential device applications. Electrons localized in semiconductor crystallites of diameters ranging from 30 to 800 Å embedded in a transparent insulating matrix are confined in three dimensions.<sup>1-3</sup> Such quasi-zero-dimensional (quasi-0D) electron systems also exist in bulk alloy semiconductors due to compositional fluctuations.<sup>4</sup> Electronic motion in these systems no longer follows a well-defined energy momentum relation because the Hamiltonian of the system does not commute with the momentum operator due to potential discontinuity at the crystallite surface. The envelope wave functions in spherical coordinates  $[r, \theta, \phi]$  and eigen energies of conduction electrons and valence holes localized in an infinite spherical well within the effective mass approximation are given by

$$|nLm\rangle = C_{nLjL}(\chi_{nL}r)Y_{Lm}(\theta, \phi) \quad (1)$$

and

$$E_{nL} = \hbar^2 \chi_{nL}^2 / 2m_{e,h} a^2, \quad (2)$$

respectively, where the subscripts  $n$ ,  $L$ , and  $m$  are effective radial, angular, and magnetic quantum numbers, respectively; the  $j$  and  $Y$  are the spherical Bessel and spherical Harmonic functions, respectively;  $a$  is the radius of crystallite; and  $m_{e,h}$  is the effective mass of electron or the isotropic hole mass.<sup>5</sup> The values of  $\chi_{nL}$  for the lowest two states of either conduction electron or valence hole  $1S$  and  $1P$  are  $\pi$  and 4.49, respectively.  $S$  stands for  $L = 0$  and  $P$  for  $L = 1$ . The allowed transitions which conserve angular and radial quantum numbers are  $1S-1S$ ,  $1P-1P$ , and higher transitions. The physical picture of quasi-0D electron system described above has been experimentally verified by several groups.<sup>1-3</sup> Large and fast optical nonlinearities arising from photogenerated electron hole pairs have been reported in quasi-0D electron systems.<sup>6,7</sup>

In this letter, we report on measurements of ultrashort recombination lifetimes of the radial and angular quantum number conserved  $1S-1S$  and  $1P-1P$  transitions in quasi-0D electron systems in  $\text{CdS}_x\text{Se}_{1-x}$  at 4.3 K using a streak camera detection system. The time-resolved photoluminescence (PL) detected at various emission energies allows us to unambiguously identify the  $1S-1S$  and  $1P-1P$  transitions. The recombination lifetime of  $1P-1P$  transition was measured to be 3.5 times shorter than the  $1S-1S$  transition. The ultrafast decay of the  $1P$  excitation may have practical importance for the construction of ultrafast reversible optical switches. The

assignment of the observed  $S$  and  $P$  transitions was supported by calculations of eigen energy levels and squared matrix element ratio for these transitions, as well as the observation of optical transitions in steady-state PL.

The samples investigated were four optical glass filters Corning 2-61, 2-59, 2-58, and 2-64. The value of  $x$  for each sample was accurately obtained from chemical analysis.<sup>8</sup> A second harmonic (530 nm) of a Nd-glass laser pulse of 8 ps duration was used to excite the samples on the front surface. The maximum optical energy incident onto the front surface was about 40  $\mu\text{J}$ . The spot size was about  $8 \times 10^{-3} \text{ cm}^2$ . For steady-state PL experiments, an argon-ion laser, a Spex double grating spectrometer, an S-20 photomultiplier, and a lock-in amplifier were used.

The time-resolved PL profiles obtained at various emission energies at 4.2 K for sample 2-58 are shown in Figs. 1(a)-1(e). The left curve in Fig. 1(a) shows the temporal profile of the exciting laser pulse which reflects the time resolution of the detection system (10 ps). The dotted curves in Fig. 1 are the double-exponential fits to the data with a value of 12 ps for the rise time  $\tau_r$ . The decay times of these time-resolved luminescence profiles show only two distinct values. For emission energies ranging from 2.213 to 2.175 eV and from 2.1 to 1.967 eV the decay times are 29 and 100 ps, respectively.

The decay time as function of emitted photon energy  $E$  for four quasi-0D electron systems at 4.2 K is summarized in Fig. 2. For a comparison, the exciton lifetime versus exciton energy in a quasi-0D system in a bulk  $\text{CdS}_{0.53}\text{Se}_{0.47}$  alloy compound studied by Kash *et al.*<sup>9</sup> is also included in this figure. The most remarkable feature of interest in the data is the appearance of two distinct energy regions in which the decay time is different by a factor of about 3.5 for the samples 2-64, 2-58 and the bulk  $\text{CdS}_{0.53}\text{Se}_{0.47}$  while the other two samples do not show this feature because either  $1P$  electron and hole were not excited or the luminescence from the  $1P-1P$  electron-hole recombination was not detected. It is expected that the decay time should be nearly invariable over the energy range of emission if only the lowest confined state  $1S$  for electrons and holes is occupied. The wide spectral range most likely reflects the crystallite size distribution and the fluctuations in the value of  $x$  from crystallite to crystallite. When the two lowest states  $1S$  and  $1P$  are substantially occupied and the recombination lifetimes associated with these two states are considerably different, a steplike change of decay time will be observed in two distinct energy regions.

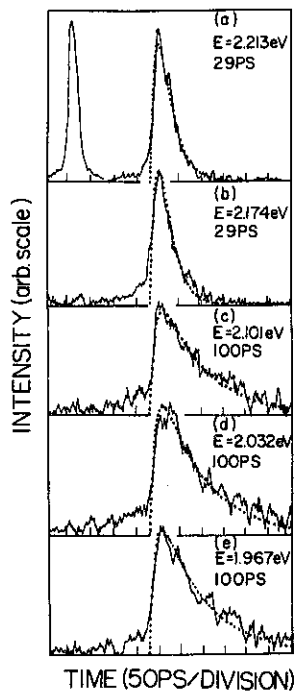


FIG. 1. Time-resolved PL profiles detected at different energies (a)–(e) for the sample 2-58 at 4.2 K. The dotted curves are the theoretical fit with 12 ps for rise time and decay times are indicated on the corresponding profiles. The left curve of (a) is the temporal response profile to the laser pulse used to excite the samples.

The exact lifetime ratio in the two energy regions depends on the transition matrix elements. The above argument should in principle explain what we observed. However, the energy dependence of localized exciton lifetime in the bulk compound  $\text{CdS}_{0.53}\text{Se}_{0.47}$  as displayed in Fig. 2(e) also exhibits a steplike feature. The explanation given by Kash *et al.*<sup>9</sup> was based on the model suggested by Cohen and Sturge<sup>4</sup> where the exciton migration goes from a site with higher energy into another site with lower energy. This raises a question whether the exciton migration mechanism can apply to the present case. Since exciton migration must involve a transport over a relatively large distance due to the nature of the exciton-phonon interaction,<sup>4</sup> such migration may occur in relatively large crystallites. This apparently may explain the results observed in samples 2-58 and 2-64. In smaller crystallites the migration does not occur in correspondence with the samples 2-61. However, the exciton migration picture

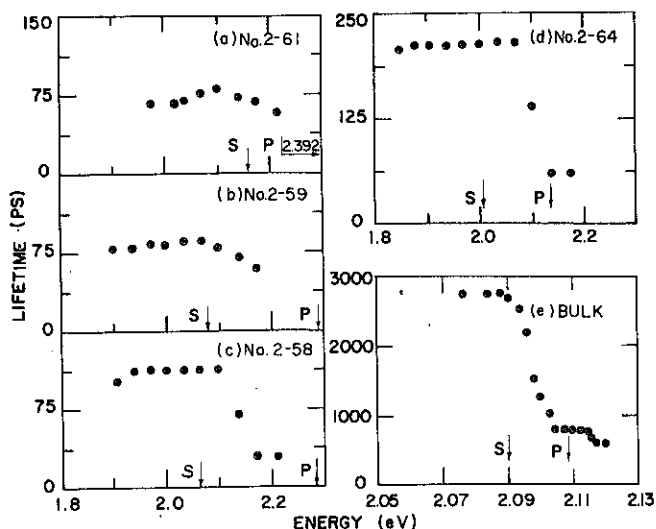


FIG. 2. Lifetimes are plotted as function of emitted photon energy. The sample temperature for (a), (b), (c), (d) is 4.2 K and for (e) is 2 K. The arrows indicate the energy positions for the  $1S-1S$  transition (S) and the  $1P-1P$  transition (P).

cannot explain the steplike energy dependence of lifetime as well as the ratio with the value of about 3.5 because the depth of a potential well caused by compositional fluctuations is entirely random in nature. Furthermore, the exciton lifetime would increase monotonically with a decrease of exciton energy.

A two-state ( $1S, 1P$ ) model is introduced here which consistently interprets all the results shown in Fig. 2 as well as other results observed by Cohen and Sturge<sup>4</sup> and reported by Kash *et al.*<sup>9</sup> It is possible that the excitons are confined by the potential wells in the bulk alloy compound which have two lowest states designated by  $1S$  and  $1P$ . The exciton in higher lying state  $1P$  can be scattered to the lower lying state  $1S$  by emission of phonons instead of migrating from site to site.

In order to verify the two-state model, we have calculated the eigen energy levels of the quasi-0D electron systems and the recombination lifetime ratio for  $1S-1S$  and  $1P-1P$  transitions. The confinement energy for the ground states ( $E_{1S}^e$ ) is equal to  $E_{1S}^e + E_{1S}^h$  for the quasi-0D electron systems, where  $E_{1S}^e$  and  $E_{1S}^h$  are the lowest confinement energies for electrons and holes, respectively. These energies were calculated from the bulk band gaps<sup>10</sup> at 300 K and the measured peak energies of the first derivative of room-temperature reflectance ( $dR/d\lambda$ ) by subtraction. Using the electron effective mass, the isotropic hole effective mass given in Ref. 4, and the measured  $E_{1S}$ , the effective diameter of crystallite for each sample and eigen energies were calculated based on Eq. (2) and listed in Table I. The emitted photon energies at 4.2 K for  $1S-1S$  and  $1P-1P$  transitions in Table I were obtained by adding corresponding confinement energies to the values of bulk gap<sup>10</sup> at 4.2 K. These calculated energy positions are located in Fig. 2 as arrows labeled by S and P for clarity and are in reasonable good agreement with the two-state model.

The radiative lifetime ratio for  $1S-1S$  and  $1P-1P$  can be predicted following the approach given by Casey and Panish.<sup>11</sup> The matrix element for a transition from localized state in conduction band to the localized state in valence band is  $M = M_b M_{env}$ , where  $M_b$  is the average matrix element for the Bloch states for bands in absence of new eigen states due to the confinement and  $M_{env}$  is the envelope part of the matrix element which is  $M_{env} = \langle 1L | 1L \rangle$ . Since the  $1P$  state is a threefold degeneracy state with magnetic quantum number of  $-1, 0, 1$ , the envelope matrix element ratio of  $|M_{env}|_{1P-1P}^2$  to  $|M_{env}|_{1S-1S}^2$  can be readily calculated to be 5. When the 4 K recombination lifetimes are purely radiative, then the ratio for  $\tau_{1S}/\tau_{1P}$  should be equal to 5. The discrepancy between the predicted value of 5 and the experimentally measured value of 3.5 for  $\tau_{1S}/\tau_{1P}$  arises from the existence of nonradiative transitions. A simple rate equation analysis helps to substantiate this statement. Suppose  $1/\tau_{li} = 1/\tau_{ri} + 1/\tau_{ni}$ , where  $i = S, P$ ,  $\tau_{rs(p)}$  and  $\tau_{ns(p)}$  are the radiative and nonradiative recombination lifetimes for the  $1S(P)-1S(P)$  transition, respectively. The ratio is  $\tau_{1S}/\tau_{1P} = (\tau_{rs}/\tau_{rp}) [(\tau_{rp} + \tau_{np})/(\tau_{rs} + \tau_{ns})]$ . When  $\tau_{ns} \sim \tau_{np}$  and  $\ll \tau_{rs}, \tau_{rp}$ , then  $\tau_{1S}/\tau_{1P} \sim 1$ ; hence, there should be only one lifetime. This is opposite to the experimental results. On the other hand, the ratio  $\tau_{1S}/\tau_{1P}$  is about 3.5 when

TABLE I. Measured energy peak of first derivative of reflection at 300 K, bulk energy gaps at 4.2 and 300 K, the calculated confinement energies, emission energies for 1S-1S and 1P-1P transitions and effective diameters ( $d$ ), the measured lifetimes for 1S-1S and 1P-1P transitions as well as their ratio are displayed.

No.	Sample $\text{CdS}_x\text{Se}_{1-x}$ $x$	Sample effective diameter $d$ (Å)	Energy (300 K)		Confined energy (meV)					4 K emission energy <sup>a</sup> (eV)		4 K lifetime (ps)		$\tau_{1s}/\tau_{1p}$	
			Energy peak for $dR/d\lambda$ (eV)	Bulk gap <sup>a</sup> (eV)	$E_{1s}^e + E_{1s}^h$	$E_{1s}^e$	$E_{1s}^h$	$E_{1p}^e$	$E_{1p}^h$	1S-1S	1P-1P	$\Delta E^b$	1S		1P
2-61	0.27	74	2.0120	1.7857	226	187	39	382	80	2.156	2.392	220	70	20 <sup>d</sup>	3.5
2-59	0.121	80	1.9366	1.7333	203	168	35	344	72	2.078	2.291	224	85	24 <sup>d</sup>	3.5
2-58	0.081	80	1.9245	1.7143	210	174	36	356	74	2.065	2.284	c	100	29	3.5
2-64	0.168	102	1.8666	1.7429	124	103	21	211	43	2.004	2.134	c	210	60	3.5
Bulk	0.530	250		1.9368	17	14	3	29	6	2.090	2.108		2750	790	3.5

<sup>a</sup> From Ref. 10.

<sup>b</sup> Measured energy separation (meV) between S and P peaks at 300 K from Fig. 3(a).

<sup>c</sup> Peaks are broad and unresolved.

<sup>d</sup> The anticipated values assuming a same ratio  $\tau_{1s}/\tau_{1p}$  for the samples 2-58 and 2-64.

nonradiative recombination lifetimes ( $\tau_{ns} = \tau_{np}$ ) are about 5 times larger than the radiative lifetime  $\tau_{rp}$  of the excited state 1P for the assumption of  $\tau_{1p} \sim \tau_{rp}$  and  $\tau_{1s} \sim \tau_{rs}$ .

Steady-state PL studies at 4 and 300 K were performed to substantiate our findings from the picosecond studies. In Fig. 3(a), 300 K PL spectra of sample 2-61 at various excitation levels (see figure caption) are plotted. The broken vertical line indicates the peak position of  $dR/d\lambda$ . As expected the salient feature in the luminescence spectra is the appearance of a two-peak structure separated by 220 meV on the high-energy side of the broken vertical line. Based on the two-state model we attribute these two peaks to the 1S-1S and 1P-1P optical transitions<sup>5</sup> as indicated by S and P in the figure.

The 4 K PL spectrum of 2-61 excited by the 457.9-nm line of the argon-ion laser is depicted in Fig. 3(b). As can be seen from the spectrum, the position of the 1S-1S peak shifts to higher energy and its FWHM (58 meV) decreases by a

factor of 2 in comparison with room-temperature data. The latter indicates that the broadening of the 1S-1S transition at room temperature is not entirely dominated by the size fluctuation. The inset of Fig. 3(b) shows a spectrum fit by assuming a Gaussian shape of the probability density function for the random variable  $d$ . The fit gives a mean value of 74 Å for the effective diameter and a full width at half-maximum of 15 Å which characterizes the size fluctuation of microcrystallites. The structure next to the main 1S-peak is from the 1P-1P transition since its energy separation with the 1P peak is about 210 meV.

We have also measured 4 and 300 K luminescence spectra of 2-59, 2-58, and 2-64 samples. The two-peak structure was observed for 2-59 at both 4 and 300 K. The peaks were broader for 2-58 and 2-64 than for the other two samples and the 1P structure was not clearly identified.

In summary, we have reported on the measurements of recombination lifetimes of 1S-1S and 1P-1P transitions in quasi-0D electron systems in  $\text{CdS}_x\text{Se}_{1-x}$ . The assignment to these observed transitions is supported by calculations of eigen energy levels and the corresponding squared matrix element ratio as well as the direct observation of optical transitions between quantized energy levels 1S and 1P in the conduction band and the valence band.

This work was supported by Air Force Office of Scientific Research AFOSR-86-0031.

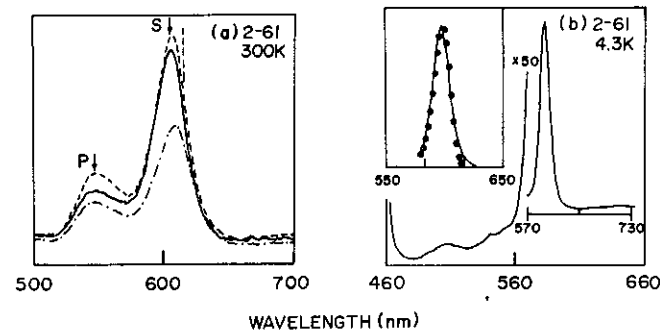


FIG. 3. (a) Photoluminescence spectra of sample 2-61 at various excitation levels taken at room temperature using the 488 nm line of an argon-ion laser. The excitation levels (intensity scale) were 2.5 (2) and 10 (10) times higher for the broken curve and the dot-dashed curve than the solid curve, respectively. The broken vertical line indicates the peak position of the first derivative of reflectance at room temperature. S and P stand for the 1S-1S and 1P-1P transitions, respectively. (b) Photoluminescence spectra of 2-61 at 4.3 K. The inset shows that the 1S peak broadening is dominated by the diameter fluctuation of microcrystallites. The solid dots are calculated by assuming a Gaussian shape of the probability density function for the random variable  $d$  with a variance of 25 Å<sup>2</sup>.

<sup>1</sup>R. Rossetti, S. Nakahara, and L. E. Brus, *J. Chem. Phys.* **79**, 1086 (1983).

<sup>2</sup>A. I. Ekimov and A. A. Onushchenko, *JETP Lett.* **40**, 1136 (1984).

<sup>3</sup>J. Warnock and D. D. Awschalom, *Phys. Rev. B* **32**, 5529 (1985); *Appl. Phys. Lett.* **48**, 425 (1986).

<sup>4</sup>E. Cohen and M. D. Sturge, *Phys. Rev. B* **25**, 3828 (1982).

<sup>5</sup>L. E. Brus, *IEEE J. Quantum Electron.* **QE-22**, 1909 (1986).

<sup>6</sup>R. K. Jain and R. C. Lind, *J. Opt. Soc. Am.* **73**, 647 (1983).

<sup>7</sup>S. S. Yao, C. Karaguleff, A. Gabel, R. Fortenberry, C. T. Seaton, and G. I. Stegeman, *Appl. Phys. Lett.* **46**, 801 (1985).

<sup>8</sup>The samples were sent to Schwarzkopf Microanalytical Laboratory, Inc. (56-19 37th Ave., Woodside, NY 11377) for chemical wet analysis to obtain accurate  $x$  values.

<sup>9</sup>J. A. Kash, A. Ron, and E. Cohen, *Phys. Rev. B* **28**, 6147 (1983).

<sup>10</sup>F. L. Pedrotti and D. C. Reynolds, *Phys. Rev.* **127**, 1584 (1962).

<sup>11</sup>H. C. Casey, Jr. and M. B. Panish, *Heterostructure Lasers* (Academic, New York, 1978), p. 144.